

# Water Defect and Pore Formation in Atomistic and Coarse-Grained Lipid Membranes: Pushing the Limits of Coarse Graining

W.F. Drew Bennett<sup>†</sup> and D. Peter Tieleman<sup>\*,†</sup>

<sup>†</sup>Department of Biological Sciences and Institute for Biocomplexity and Informatics, University of Calgary, 2500 University Drive N.W., Calgary, Alberta T2N 1N4, Canada

 Supporting Information

**ABSTRACT:** Defects in lipid bilayers are important in a range of biological processes, including interactions between antimicrobial peptides and membranes, transport of polar molecules (including drugs) across membranes, and lipid flip–flop from one monolayer to the other. Passive lipid flip–flop and the translocation of polar molecules across lipid membranes occur on a slow time scale because of high-energy intermediates involving water defects and pores in the membrane. Such defects are an interesting test case for coarse-grained models because of their relatively small characteristic size at the level of water molecules and the complex environment of water and polar head groups in a low-dielectric membrane interior. Here we compare coarse-grained simulations with the MARTINI model with the standard MARTINI water and two recently developed coarse-grained polarizable water models to atomistic simulations. Although in several cases the MARTINI model reproduces the correct free energies, there are structural differences between the atomistic and coarse-grained models. The polarizable water model improves the free energies but only moderately improves the structures. Atomistic test simulations in which water molecules are artificially tethered to each other in groups of four, the resolution of MARTINI, suggest that the limiting factor is not the size of the coarse-grained particles but rather the simple interaction potential and/or the entropy lost in coarse graining the system. By increasing the attractive interaction between the lipids' headgroup and water, we did observe pore formation but at the expense of the correct equilibrium properties of the bilayers.

## INTRODUCTION

Biological membranes form the boundaries of cells and organelles. They regulate what can enter and leave a cell, communicate signals across the membrane, provide structural support, localize distinct chemical environments, and allow electrochemical gradients, which are necessary for energy transduction and nerve propagation. The core structure of membranes, the lipid bilayer, consists of a thin (3 nm) hydrophobic slab that forms a semipermeable membrane, preventing ions, polar and charged molecules, from crossing. Several biologically important processes involve the interactions of polar or charged molecules and lipid bilayers. A few examples are electroporation, where an applied electric field induces hydrophilic pores in membranes; antimicrobial peptides, which have been shown to cause pore formation;<sup>1</sup> lipid translocation; and drug delivery. The interaction between a membrane and polar molecules depends on its lipid composition, which varies significantly between cell types and organelles.<sup>2</sup>

Lipid translocation, or flip–flop, between monolayers is an important process in cells. It involves a high free energy barrier for polar and charged lipid head groups crossing the hydrophobic bilayer interior. Flip–flop is important for the growth of membranes as well as cellular signaling.<sup>3</sup> The rate of passive flip–flop for PC and other phospholipids is very slow, on the time scale of hours to days.<sup>4–6</sup> The mechanism of PC flip–flop has been shown to involve pore formation,<sup>4,7,8</sup> with water and other lipid head groups entering the hydrophobic bilayer interior to prevent the dehydration of the flipping lipids headgroup. Other polar and charged molecules have been shown to disrupt

the lamellar structure of the bilayer causing water defects,<sup>9,10</sup> where water and head groups enter the bilayer interior from only one side of the bilayer.

We are investigating the mechanism, thermodynamics, and kinetics of the process of lipid flip–flop and pore formation using computer simulations.<sup>9,10</sup> The standard approach uses a force field that describes interactions at the level of individual atoms (AA for all-atom). Typical trajectories on systems with ca. 20 000 atoms can reach a time scale on the order of a microsecond. More recently, a number of coarse-grained (CG) models have been developed that retain some chemical specificity but operate at a lower level of resolution. We use the MARTINI model,<sup>11</sup> in which typically four nonhydrogen atoms are grouped together into a single interaction site. This allows simulations on a scale that is 2–3 orders of magnitude larger than AA simulations with a comparable computational cost, but achieving a balance between detail and computational efficiency is a substantial challenge. There is a strong motivation to have a CG model that can reproduce both the energetics and the mechanism of membrane pores and defects.

MARTINI maps four water molecules to a single water bead, without a dipole or partial charge. One limitation of such a model is its inability to reproduce small-scale defects, for instance during lipid flip–flop.<sup>11</sup> A recently developed MARTINI water model<sup>12</sup> (CG-pol) combines four water molecules into three beads that represent a dipole. CG-pol simulations show pores in

Received: April 27, 2011

Published: August 04, 2011

membranes during electroporation, in agreement with AA simulations.<sup>12</sup> This suggests CG-pol might be better suited to study lipid translocation. The recently developed BMW water model for MARTINI uses a modified Born–Mayer–Huggins potential, which is softer than the standard Lennard-Jones potential.<sup>13</sup> This model was shown to reproduce the lipid interface dipole potential, which suggests it could be a useful model for heterogeneous interfacial systems.

In previous studies we have calculated atomistic potentials of mean force (PMFs) for lipid flip–flop in a number of bilayers with primarily PC lipids, including varying chain length,<sup>8</sup> cholesterol concentration,<sup>14</sup> chain unsaturation<sup>8</sup> and the effect of a the presence of a simple transmembrane helix on lipid flip–flop.<sup>15</sup> Here we describe simulations of phospholipid flip–flop using five different models (AA, AA-bundled, CG, CG-pol, and CG-BMW) in three different membranes: dilauroylphosphatidylcholine and dipalmitoylphosphatidylcholine (DLPC and DPPC, respectively), which in MARTINI differ by one bead in each acyl chain, and the charged lipid dioleoylphosphatidylglycerol (DOPG) in a dioleoylphosphatidylcholine (DOPC) bilayer. CG-pol improves the results most for DOPG, although the structure of the defects is different between atomistic and CG models in all cases. CG simulations of flip–flop in DLPC give a much higher barrier than in atomistic simulations. To understand the possible effect of the larger size of MARTINI particles, in particular the water particles that group four water molecules into one, we simulated AA dimyristoylphosphatidylcholine (DMPC) with normal water and with water tethered in groups of four,<sup>16</sup> with no discernible effect on either structure or free energies. Finally, we tested different parameters for the MARTINI model to see if pore formation was possible with a CG model. By increasing the interaction between water and lipid head groups in the CG-pol model, we did observe pore formation in the DLPC bilayer. These results provide insight for future progress in refining CG lipid models.

## METHODS

**AA Simulations.** We used the GROMACS software package.<sup>17</sup> For lipid parameters we used the united-atom Berger force field.<sup>18</sup> We use a relatively small bilayer patches of 64 lipids for DLPC, DPPC, and DOPC bilayers. We include between ca. 4000 and 5000 simple point charge (SPC)<sup>19</sup> water molecules for good hydration of the lipid head groups. Small bilayers are necessary for free energy calculations, which require 40–50 replicates for 10–100 ns to determine a single PMF (see Umbrella Sampling Section). To test the effect of using small bilayers for simulating large-scale changes in the bilayer structure during flip–flop, we determined a PMF for DMPC with 256 lipids and compared it to the PMF with 64 lipids (Figure S1, Supporting Information). The PMFs for the large and small bilayer were quite similar, indicating our small bilayer patches are sufficiently large for this process. All simulations were run at 323 K for comparison with DPPC, which has a high melting temperature (314 K).<sup>20</sup> A time step of 2 fs was used for the equations of motion. SETTLE<sup>21</sup> was used to constrain water bonds and angles, while LINCS<sup>22</sup> was used for the lipid bonds. We used periodic boundary conditions with a semi-isotropic pressure coupling algorithm with a reference pressure of 1 bar and a  $4.5 \times 10^{-5}$  bar<sup>-1</sup> compressibility.<sup>23</sup> Temperature is maintained with a weak-coupling scheme and a coupling constant of 0.1 ps.<sup>23</sup> We use the particle mesh Ewald (PME) method for

long-range electrostatic interactions with a fourth-order spline and a 0.12 nm grid spacing.<sup>24,25</sup>

The bundled water topology was from,<sup>16</sup> where four SPC waters are tethered together using harmonic distance restraints into a roughly tetrahedral geometry. A force constant of 1000 kJ mol<sup>-1</sup> nm<sup>-2</sup> and a distance of 0.3 nm were used. The Lennard-Jones C<sub>12</sub> parameter was also increased for the interaction between all the water oxygens.

**CG Simulations.** For CG simulations, we use the MARTINI model<sup>11</sup> and the recently developed polarizable MARTINI water model (CG-pol).<sup>12</sup> We used a 20 fs time step and updated the neighbor list every 10 steps. Lennard-Jones interactions were shifted from 0.9 to 1.2 nm. A Coloumbic function was used for electrostatic interactions with a dielectric constant of 15 for explicit screening. For the CG-pol model, we have used mostly the same run parameters as standard MARTINI, with the exception of the dielectric coefficient, which is 2.5 instead of 15.<sup>12</sup> We have used the same types of lipids as the AA simulations. Small bilayer patches were used with 72 DLPCs, 72 DPPCs, and 70 DOPCs with 2 DOPGs. In the CG-pol model electrostatic interactions play a more important role, so we also tested the simulations with PME instead of the standard shifted Coulomb cutoff.

We tested the recently developed BMW water model with DLPC and DPPC MARTINI bilayers.<sup>13</sup> Of note, the angle potential is modified for the lipid tails for use with the BMW water model, with the force constant reduced from 25 to 10 kJ mol<sup>-1</sup> rad<sup>-2</sup>. BMW simulations were run with PME for long-range electrostatics with a 0.2 nm grid spacing and sixth-order spline interpolation.<sup>24,25</sup>

In the CG-pol model, the Lennard-Jones interaction between water beads and the choline and phosphate was reduced compared to standard MARTINI, to compensate for the increased Coulombic interactions. To try and induce pore formation, we increased the Lennard-Jones interaction between water beads and the choline and phosphate beads. For CG-pol, we increased the interaction back to the level in standard MARTINI (with  $\epsilon = 5.6$  kJ/mol for both interactions, compared to 5 and 4.5 kJ/mol for phosphate–water and choline–water in CG-pol). We refer to this model as CG-pol-lj\*. We also increased the Lennard-Jones interaction between water and the head groups in standard MARTINI (CG-lj\*) to levels beyond the range of the MARTINI force field (with  $\epsilon = 6.2$  kJ/mol). We then determined PMFs for DLPC and DPPC flip–flop using the CG-pol-lj\* model and for DLPC using the CG-lj\* model.

**Umbrella Sampling.** With current computers, we are able to simulate up to 1  $\mu$ s for the AA model and to the 100  $\mu$ s and nearly millisecond time scale for the CG model. The time scale of phospholipid flip–flop is hours to days. To simulate these slow processes, we use umbrella sampling. We run a series of ca. 50 simulations in parallel with a harmonic restraint placed on the headgroup of the translocating lipid with respect to the distance from the center of the bilayer, spaced by 0.1 nm increments. The harmonic restraint is placed on the polar or charged headgroup to ensure that the molecule samples the center of the bilayer, which is likely to be energetically unfavorable. We determine the PMF using weighted histogram analysis.<sup>26</sup> In each system, we pull two separate lipids, staggered by at least 4 nm, to increase computational efficiency by getting two PMFs at a time. We have determined the PMF for a single DPPC lipid, and it was within the error of the PMF calculated by pulling two DPPC lipids (Figure S2, Supporting Information). We plot the mean from the

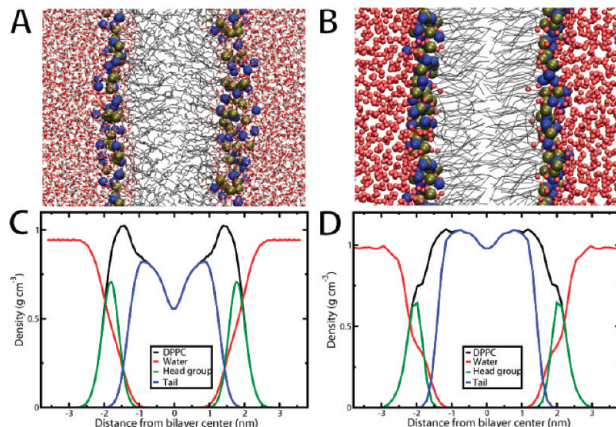


**Figure 1.** Snapshot and partial density profile for an AA (A and C) and CG (B and D) DPPC bilayer at equilibrium. Water is shown as small balls, head groups as thick balls, and lipid tails as thin lines. Head group includes the choline and phosphate groups, and tails include all the carbons after the carboxyl group.

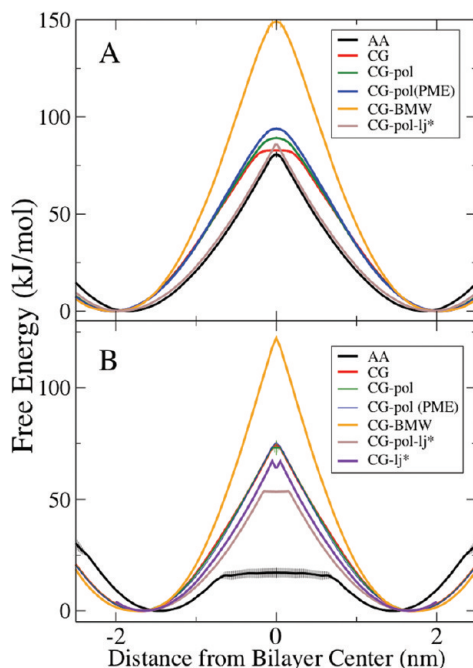


**Figure 2.** PMFs for phospholipid flip-flop. (A) DPPC flip-flop in a DPPC bilayer. (B) DLPC flip-flop in a DLPC bilayer. Error bars represent the standard error between two independent lipids PMFs. The PMF is mirrored at the center of the bilayer for clarity. The CG, CG-pol, and CG-pol (PME) PMFs are nearly the same, so only one curve is visible.

two independent PMFs and the standard error, after aligning the PMFs to zero at their free energy trough. In all the figures, we have shown the PMF and its mirror image that corresponds to the opposite leaflet. As the bilayers are all symmetric, the PMFs should be the same in both monolayers.

## ■ RESULTS

**Phospholipid Flip-flop.** Figure 1A and B shows snapshots of AA and CG DPPC lipid bilayers. Figure 1C and D shows the partial density profiles for the two bilayers. Water penetrates into

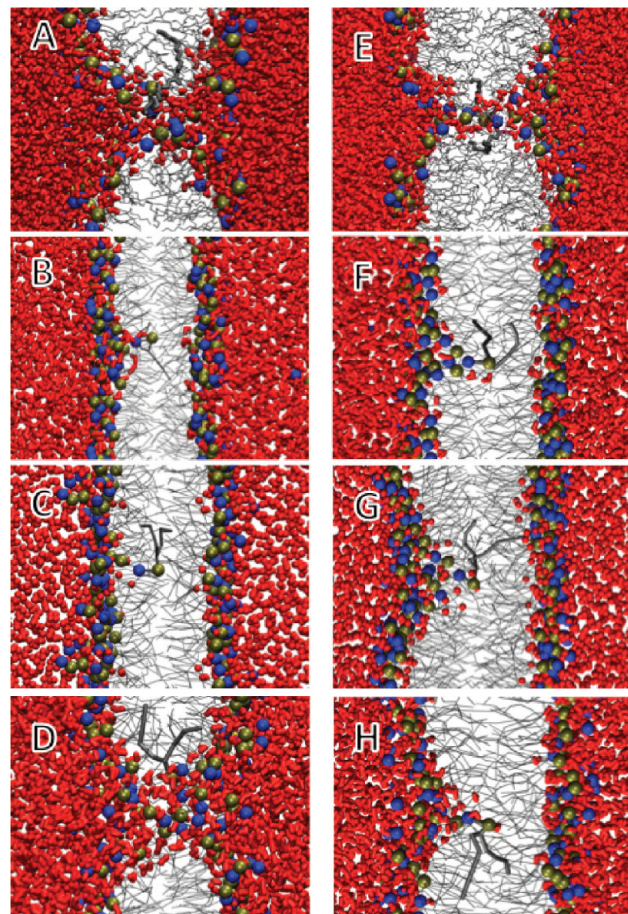


**Figure 3.** Snapshots for a phospholipid restrained at the center of bilayers. Water is shown as red licorice, lipid tails as gray lines, restrained lipid as thick gray lines, and headgroup phosphate (phosphorus) and choline (nitrogen) as balls. (A) and (E) are atomistic, (B) and (F) are CG-pol, (C) and (G) are CG, and (D) and (H) are CG-pol-lj\* simulations. (A–D) DLPC in a DLPC bilayer and (E–H) DPPC in a DPPC bilayer.

the headgroup region and a small amount into the carbon tail density. This is followed by an increase in the tail density until a maximum, after which the density decreases near the center of the bilayer. The CG model reproduces the general features of the density profile, although the CG model does not have as large of a decrease near the bilayer center compared to the AA model.

DPPC. Figure 2A shows the PMF for AA DPPC flip-flop.<sup>4</sup> We used umbrella sampling (see Methods Section) to determine the free energy profile for transferring a single DPPC from equilibrium to the center of the bilayer, with umbrellas centered on the phosphate group. There is a large free energy trough corresponding to the equilibrium position of the phosphate in the bilayer (Figure 2). Moving the lipid into the bilayer has a large free energy cost.

As we move the phosphate of DPPC into the hydrophobic bilayer core, a water defect forms. Water and other PC lipid head groups move into the bilayer to prevent the DPPC from becoming desolvated. Restraining the zwitterionic headgroup of DPPC inside the bilayer significantly perturbs the lamellar structure. Similar structures and free energy slopes have been observed for other charged and polar molecules entering the interior of lipid bilayers.<sup>7,27,28</sup> When the phosphate is restrained

at the center of the bilayer, a pore spanning the bilayer is observed (Figure 3E). We assume this is the transition state for lipid flip-flop. Estimates for the lifetime of pores are on the order of 10–100 ns.<sup>29</sup> From the free energy barrier for pore formation (80 kJ/mol) and the flux of lipids across a preformed pore, a rate for DPPC flip-flop was estimated to be 4–30 h, in good agreement with experimental estimates of 1–90 h.<sup>5,6</sup>

The PMF for CG DPPC flip-flop shows a similar shape as the AA model (Figure 2A) and has a similar barrier for flip-flop. As the DPPC is moved into the bilayer, a small water defect does form, corresponding to a steep free energy slope. No water pore is observed when the phosphate bead is restrained at the bilayer center, although a small, unstable water defect does occasionally form (Figure 3G).

We have also determined a PMF for DPPC flip-flop using the CG-pol model (Figure 2A). Compared to the nonpolarizable model, the shape of the PMF and the free energy barrier are quite similar. Figure 3F shows that a small water defect is formed when the phosphate is at the bilayer center, although a pore is still not observed. The defects formed for CG-pol occur more often and appear slightly more stable than for CG. We determined the number of contacts (distance of less than 1 nm) formed between water beads and the phosphate bead restrained at the center of the bilayer. For CG, 98% of the time there were no contacts, 1.2% with one contact, and a maximum of 4 contacts. There were no contacts for the CG-pol model 92% of the time, 6% with one contact, 2% with two contacts, and a maximum of 7 contacts. The use of PME makes almost no difference.

To try and induce pore formation, we increased the Lennard-Jones interaction between the water bead and the choline and phosphate beads (CG-pol-lj<sup>\*</sup>). Coincidentally, the PMF for CG-pol-lj<sup>\*</sup> is nearly the same as the AA model, although the bilayers bulk properties were perturbed significantly. The area per lipid for the DPPC CG-pol model was 0.64 and 0.71 nm<sup>2</sup> for the CG-pol-lj<sup>\*</sup> model. For CG-pol-lj<sup>\*</sup>, the water defect was more stable, although we did not observe pore formation. When the phosphate of DPPC was restrained at the bilayer center, there were 2–5 contacts between the phosphate and the water for 80% of the simulation.

The BMW water model has a steeper slope in the PMF and a significantly higher barrier for flip-flop (150 kJ/mol), although the position of the free energy minima is the same as the other two CG models. At the center of the bilayer there was 1 contact with water and the phosphate for 49% of the time, 2 contacts for 48%, and a maximum of 5 contacts. No pores are observed for the BMW DPPC simulations.

**DLPC.** From the AA model, shorter lipids, such as DLPC, had lower free energy barriers for pore formation compared to DPPC. Figure 2B shows the PMF for DLPC. Similar to DPPC, there is a free energy trough at DLPC's equilibrium position and a steep slope as the PC headgroup moves into the bilayer center, corresponding to water defect formation. When the lipid was ca. 0.6 nm from the bilayer center, the water defect became a pore, causing the PMF to plateau. Once a pore forms, the lipid is able to diffuse across it at no free energy cost. This indicates that pore formation is the primary free energy barrier for flip-flop. Figure 3A shows the water pore formed at the center of the DLPC bilayer, which has many lipid head groups and water molecules in the bilayer interior. From the AA model, we calculate a free energy barrier for DLPC flip-flop of 16 kJ/mol. This low free energy barrier translates into a rate of flip-flop on the  $\mu$ s time scale.<sup>8</sup>

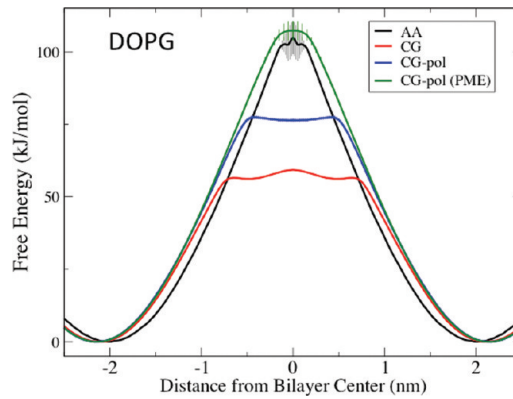


**Figure 4.** PMFs for DOPG flip-flop in a pure DOPC bilayer. Error bars are shown and represent the standard error between two independent lipids PMFs. The PMF is mirrored at the center of the bilayer for clarity.

Using the CG and CG-pol model, we calculated the PMF for DLPC flip-flop in a DLPC bilayer (Figure 2B). The PMFs for DLPC flip-flop are the same for the CG, CG-pol, and CG-pol with PME. There is a deep free energy minimum and a large, smooth increase in free energy to the center of the bilayer. The free energy barrier for DLPC flip-flop is 73 kJ/mol. Similar to the DPPC PMF, the BMW DLPC PMF has both a steeper slope and a higher barrier for flip-flop (122 kJ/mol). The steep slope of the PMF at the bilayer center and the snapshots (Figure 3B and C) indicate that even when the phosphate is at the center of bilayer, the lipid is still interacting with one bilayer leaflet.

The large difference between the CG models and the AA model is due to pore formation in the AA model. In contrast to the AA model, we did not observe pore formation in the CG, CG-pol, or BMW bilayers (Figure 3). At the bilayer center a small water defect forms, to keep the DLPC headgroup solvated. We did observe pore formation in the CG-pol-lj<sup>\*</sup> model (Figure 3D). The structure of the pore appears similar to the AA model, with a disordered toroidal shape and multiple water and head groups within the bilayer interior. As with the AA model, once a pore formed the PMF plateaus (ca. 0.15 nm from the bilayer center), the barrier for flip-flop was reduced to 53 kJ/mol. The bulk properties of the DLPC bilayer are modified by the use of the increased interaction between water and lipid head groups, with the area per lipid increasing from 0.62 to 0.71 nm<sup>2</sup>. We tested the CG-lj<sup>\*</sup> model but did not observe pore formation, and the PMF was similar to the CG model (Figure 2B). Pores were not observed when we only increased the phosphate–water interaction, not the choline–water interaction (data not shown). Pores were not observed by increasing the charge on the phosphate and choline in DLPC to -2 and +2 (data not shown). In a subtler attempt, we increased the repulsion between the lipid tails and the lipid head groups, but pores were not observed (data not shown).

**DOPG.** To see the effect of a charged headgroup, we calculated PMFs for DOPG flip-flop across a DOPC bilayer (Figure 4). For the AA model, the free energy barrier for DOPG (105 kJ/mol) flip-flop in a DOPC bilayer increased compared to DOPC (87 kJ/mol) in a DOPC bilayer.<sup>15</sup> At the center of the bilayer, DOPG formed a water defect, and a pore was not observed (Figure 5A); this is similar to DOPC flip-flop, where we did not observe pore formation, but a water defect was present. The PMF for CG-pol DOPG flip-flop in a DOPC bilayer is shown in Figure 4. The shape of the PMF closely matches the AA PMF

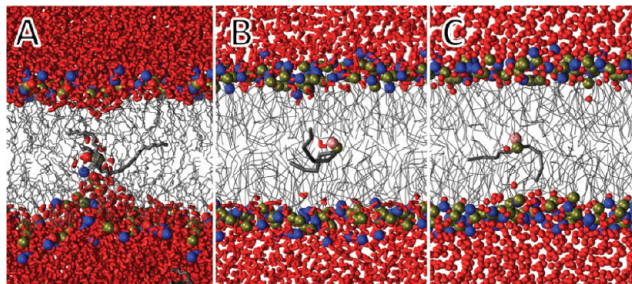


**Figure 5.** Snapshots for DOPG restrained at the center of a DOPC bilayer. Water is shown as red licorice, lipid tails as gray lines, restrained lipid as thick gray lines, and headgroup phosphate (phosphorus) and glycerol (oxygen) as balls. (A) AA, (B) CG, and (C) CG-pol simulations.

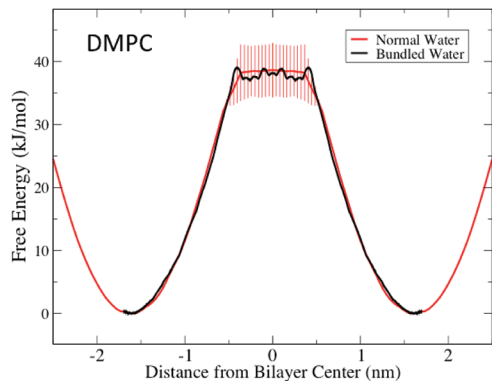


**Figure 6.** PMFs for DMPC flip–flop in a DMPC bilayer using normal SPC water and bundled water. Error bars for the normal water represent the standard error between two independent lipids PMFs. The bundled water PMF was only calculated once, so no error bars are shown. The PMF is mirrored at the center of the bilayer for clarity.

until ca. 0.6 nm, where the PMF suddenly flattens. A water defect was observed before this position, but near the center of the bilayer, a defect does not form (Figure 5B). In contrast to DLPC, where the PMF plateau was caused by pore formation, the plateau for DOPG is due to the lipid losing contact with either leaflet and with no net force in either direction, and the lipid almost completely desolvated. Occasionally a single water bead enters the bilayer to interact with the charged PG headgroup. The PMF for DOPG flip–flop across a DOPC bilayer using the CG model is shown in Figure 4. The PMF matches the shape of the CG-pol PMF, until ca. 0.75 nm from the center where it plateaus. Again, the plateau region corresponds to water defects breaking, exposing the DOPG to the bilayer interior along with an occasional single water bead (Figure 5C). The free energy barrier for DOPG flip–flop was closer to the AA model (104 kJ/mol) for the CG-pol model (77 kJ/mol) than for the CG model (59 kJ/mol). When PME was used with the CG-pol model, the resulting barrier is almost the same as for the AA model, although no stable water defect at the center of the bilayer is observed.

**Effect of Bundling Water in AA Simulations.** In all cases tested, the CG models show significantly less complex defects and in particular do not easily form pores, although the PMFs for lipid flip–flop are quite similar between CG and AA for DPPC lipids. We hypothesized that a limiting factor may be the relatively small scale of the defects: they typically involve only

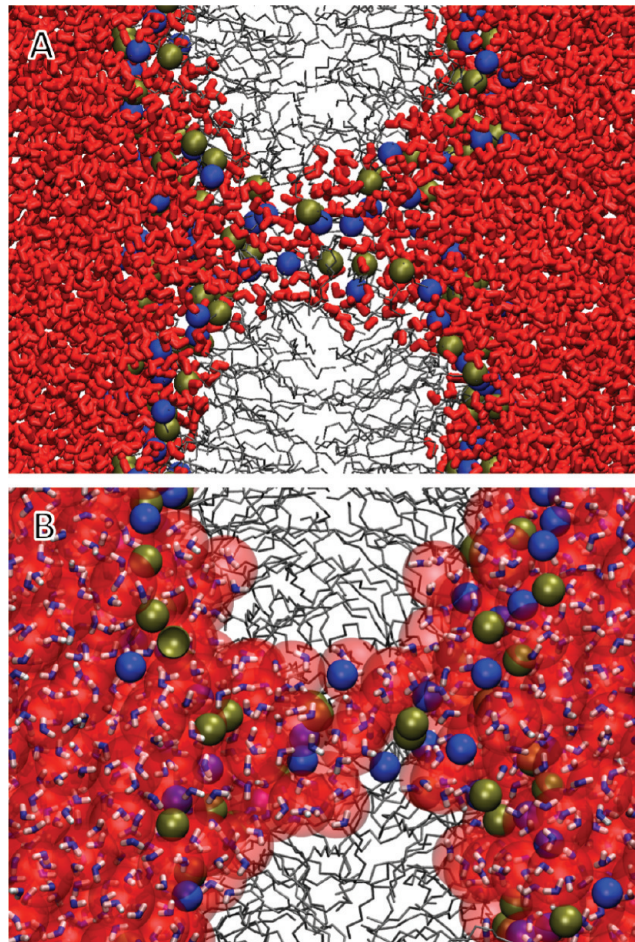


**Figure 7.** Snapshots of a pore formed in AA DMPC bilayer with (A) SPC water and (B) bundled water. The representation for (A) is the same as in Figure 3. For panel (B), bundled water is shown as blue and white licorice, with a red sphere around the four water molecules that comprise one bundled water.

a small number of head groups with associated water molecules, so that the standard MARTINI water particles may be too coarse to reproduce their structure. To test this, we artificially tethered four water molecules together in atomistic simulations<sup>16</sup> in a tetrahedral geometry that approximates a spherical shape. With this unusual water model we calculated again the PMF for DMPC flip–flop and compared it to the result for normal atomistic water. We chose DMPC for this because it has a well-defined transition state for flip–flop with a large two-sided defect or pore.<sup>8</sup> The results are surprising: the tethered waters give essentially the same thermodynamics and structure as normal water. Figure 6 shows the PMFs for the normal atomistic DMPC case and the DMPC bilayer with tethered water, while Figure 7 shows two snapshots.

## ■ DISCUSSION

We have studied the process of lipid flip–flop using molecular dynamics simulations with several different models. The AA model predicts that water defects or pores form as the headgroup of a phospholipid is transferred into the hydrophobic interior of a membrane. These membrane defects are hydrophilic; lined with other lipid head groups and water molecules. The free energy for

desolvating the charged or zwitterionic headgroup is higher than the cost of forming a water defect or a bilayer-spanning pore. We have observed similar behavior in the partitioning of charged and polar amino acid side chains in a DOPC bilayer.<sup>28</sup> The polar side chains formed water defects as they were moved into the hydrophobic interior, until the energy cost for desolvation was less than defect formation, causing the defect to break and the PMF to plateau. The charged side chains retained a water defect even at the center of the bilayer. Many other groups have observed similar behavior in the partitioning of polar and charged molecules using different force fields and methods.<sup>27,30–32</sup> For DPPC, the free energy barrier for lipid flip–flop was 80 (AA), 83 (CG), and 89 kJ/mol (CG-pol).

There is good agreement between the AA and CG models on the shape of the PMFs and the free energy barriers for DPPC. Both CG models observe water defects as the DPPC is moved into the bilayer core, but near the center of the bilayer, a pore does not form and the defects become unstable. The CG-pol model is more hydrated at the bilayer center, indicating an improvement over the standard MARTINI model. It is not obvious that the two models would give such similar results, and the physical properties are actually different. CG water has no dipole or polarizability, so simulations are run with a dielectric constant of 15 for implicit screening of electrostatic interactions. This means that the interaction of polar molecules is underestimated in hydrophobic environments, e.g., when a lipid headgroup is placed in the interior of a bilayer. In the AA model, with explicit water and dielectric screening, charge interactions are much stronger in an apolar medium, causing water pores to form when a DPPC is placed at the center of the bilayer. The CG-pol water model has explicit polarizability, and a dielectric of 2.5 is used, which means that the interaction between water and charged molecules is physically more realistic. Surprisingly, this has little effect on the structure of the defects, although CG-pol reproduces electroporation in a DPPC bilayer.<sup>12</sup> It is likely that the CG-pol will be useful for modeling phenomena where much larger pores are observed, such as the electroporation of membranes and antimicrobial peptides.<sup>12</sup> By increasing the Lennard-Jones interaction between the water and headgroup beads, we observed more stable water defects but still no pores in DPPC. We speculate that further increasing the interaction would cause pores to form, but changing these interactions perturbs the bilayer lamellar properties significantly.

Our results show that water pores are still not observed during DPPC flip–flop, in contrast to AA simulations. The large size of CG-pol water beads (4 to 1 mapping) might prevent the formation of the small water pores seen in AA DPPC flip–flop, where on the order of tens of waters are involved. However, tests of tethered water in a DMPC bilayer show that the main reason is unlikely to be size related. It was suggested (in ref 12) that using a different Lennard-Jones potential (currently a 12–6 potential), particularly a less repulsive form, might improve the model. As the CG beads become more repulsive, a larger volume would be needed to from a defect or pore, which could affect the energetics of pore formation. A less repulsive model would allow beads to get closer together, possibly making defects form more easily. To this end, we tested the BMW water model, which uses a softer potential, but found that the free energy barriers for DPPC and DLPC flip–flop are significantly overestimated. There was slightly more water pulled into the center of the DPPC bilayer using the BMW model, but again no pore formation or stable water defect was observed. The high barrier for the BMW model

is likely due to a high line tension, which would prevent pore formation.<sup>33</sup> Similarly the lack of pore formation in the CG and CG-pol model could be related to the models high bending modulus, which was shown to be nearly double atomistic and experimental values.<sup>34</sup> Although there is no immediate link between the bending modulus and the water/lipid line tension on the one hand and individual atomistic or MARTINI interactions on the other, it is likely that both properties are linked to the cost of defect formation. If future versions of MARTINI or other CG models improve these mechanical properties in a more integrated approach, then it will be interesting to see if this also results in an improved representation of membrane defects.

The CG and CG-pol models give similar results for DLPC flip–flop, and the use of PME had no effect on the energetics of flip–flop. There is a large discrepancy between the AA barrier for DLPC flip–flop (16 kJ/mol) and both CG models (73 kJ/mol). Intuitively, we expect defects and pores should form more readily in the thinner DLPC bilayer, compared to the DPPC. Experimental evidence has shown that pore formation in thin DLPC bilayer occurs spontaneously<sup>35</sup> and suggests our low free energy barrier from the AA model is realistic. Experiments on the permeation of protons and potassium ions through liposomes of monounsaturated PC lipids showed that lipids with 14 carbon tails had 2 orders of magnitude faster permeation than 18 carbon tails, which fit a pore-mediated model.<sup>36</sup> Increasing the interaction between the headgroup and water beads caused pore formation in the CG-pol-lj\* DLPC bilayer. This suggests that neither the size of the large CG water nor the 'hard' potential for the MARTINI model prevents pore formation. As expected, increasing the water–headgroup interaction caused the area per lipid to increase, which illustrates the difficulty in parametrizing a CG force field.

We observed the largest difference between CG and CG-pol lipid PMFs for DOPG flip–flop in a DOPC bilayer. This is likely due to DOPG having a negative charge, while PC lipids are zwitterionic. The CG-pol model forms water defects to the DOPG until it is ca. 0.5 nm from the bilayer center, compared to ca. 0.75 nm for the CG model. This results in an 18 kJ/mol difference in the free energy barriers for flip–flop. Near the center of the bilayer neither model shows a water defect, although an occasional water bead does enter the bilayer to interact with the headgroup, in contrast to the AA model where a defect is present at the center. With PME, the resulting energies are very similar for both AA and MARTINI CG-pol. The use of PME with standard MARTINI has been shown to improve accurately modeling dendrimer<sup>37</sup> and antimicrobial peptide<sup>38</sup> interaction with membranes.

Given the coarseness of the MARTINI model and the complex process at length scales of a few atoms of lipid flip–flop and pore formation, the similarity in the PMFs is encouraging, although our results do suggest further refinement is necessary. These results suggest caution in using and interpreting results on polar and charged interactions with bilayer interiors, such as studies on drug partitioning, electroporation, and antimicrobial peptides, with CG models. Due to the computational demands of AA simulations and umbrella sampling calculations, it is useful to have a CG model that can be used to study membrane defects and pores. It was shown that the CG-pol water model was able to form pores across bilayers and hydrophobic slabs by applying an electric field, in agreement with AA simulations.<sup>12</sup> We have compared standard MARTINI water, polarizable MARTINI water, and the BMW water model in their ability to model the

process of lipid flip-flop. We found good agreement in the free energy profiles for DPPC and DOPG flip-flop between the AA and CG models. This work suggests that during phospholipid flip-flop, the CG-pol model forms defects only slightly more readily than standard MARTINI, in closer agreement with AA simulations. The source of this mechanistic discrepancy is not clear, although we have ruled out two possible explanations: the size of the water beads and the use of a softer repulsive nonbonded potential. We did observe pore formation in a DLPC bilayer using the CG-pol-lj\* model, which shows that pore formation is possible with CG lipids. Parameterizing a lipid force field requires a delicate balance of forces, so we do not suggest that the CG-pol-lj\* is an improvement to MARTINI but rather a proof of principle. Future work into describing the molecular driving forces for AA pore formation may be necessary to fully explain the CG result. These results and similar calculations and comparisons to atomistic results could aid the parametrization of the MARTINI model and other CG lipid models.

## ■ ASSOCIATED CONTENT

**Supporting Information.** Figure S1 shows PMFs for atomistic DMPC flip-flop using a 64 lipid and 256 lipid bilayer. Figure S2 shows PMFs with one and two restrained lipids per simulation for atomistic DPPC flip-flop. This information is available free of charge via the Internet at <http://pubs.acs.org/>.

## ■ AUTHOR INFORMATION

### Corresponding Author

\*E-mail: tieleman@ucalgary.ca.

## ■ ACKNOWLEDGMENT

This work was supported by the Natural Sciences and Engineering Research Council (NSERC). W.F.D.B. is supported by studentships from NSERC, the Alberta Heritage Foundation for Medical Research (AHFMR), and the Killam Trust. D.P.T. is an AHFMR Scientist. We thank Dr. Siewert-Jan Marrink for useful comments on the manuscript.

## ■ REFERENCES

- (1) Epand, R. M.; Vogel, H. J. Diversity of antimicrobial peptides and their mechanisms of action. *Biochim. Biophys. Acta* **1999**, *1462*, 11–28.
- (2) van Meer, G.; Voelker, D. R.; Feigenson, G. W. Membrane lipids: where they are and how they behave. *Nat. Rev. Mol. Cell Biol.* **2008**, *9*, 112–124.
- (3) Daleke, D. L. Regulation of phospholipid asymmetry in the erythrocyte membrane. *Curr. Opin. Hematol.* **2008**, *15*, 191–195.
- (4) Tieleman, D. P.; Marrink, S. J. Lipids out of equilibrium: energetics of desorption and pore mediated flip-flop. *J. Am. Chem. Soc.* **2006**, *128*, 12462–12467.
- (5) Wimley, W. C.; Thompson, T. E. Exchange and flip-flop of Dimyristoylphosphatidylcholine in Liquid-Crystalline, Gel, and 2-Component, 2-Phase Large Unilamellar Vesicles. *Biochemistry* **1990**, *29*, 1296–1303.
- (6) De Kruijff, B.; Van Zoelen, E. J. Effect of the phase transition on the transbilayer movement of dimyristoyl phosphatidylcholine in unilamellar vesicles. *Biochim. Biophys. Acta* **1978**, *511*, 105–115.
- (7) Gurtovenko, A. A.; Vattulainen, I. Molecular mechanism for lipid flip-flops. *J. Phys. Chem. B* **2007**, *111*, 13554–13559.
- (8) Sapay, N.; Bennett, W. F. D.; Tieleman, D. P. Thermodynamics of flip-flop and desorption for a systematic series of phosphatidylcholine lipids. *Soft Matter* **2009**, *5*, 3295–3302.
- (9) Marrink, S. J.; de Vries, A. H.; Tieleman, D. P. Lipids on the move: simulations of membrane pores, domains, stalks and curves. *Biochim. Biophys. Acta* **2009**, *1788*, 149–168.
- (10) Gurtovenko, A. A.; Anwar, J.; Vattulainen, I. Defect-mediated trafficking across cell membranes: insights from in silico modeling. *Chem. Rev.* **2010**, *110*, 6077–6103.
- (11) Marrink, S. J.; Risselada, H. J.; Yefimov, S.; Tieleman, D. P.; de Vries, A. H. The MARTINI force field: coarse grained model for biomolecular simulations. *J. Phys. Chem. B* **2007**, *111*, 7812–7824.
- (12) Yesylevskyy, S. O.; Schafer, L. V.; Sengupta, D.; Marrink, S. J. Polarizable Water Model for the Coarse-Grained MARTINI Force Field. *PLoS Comput. Biol.* **2010**, *6*, e1000810.
- (13) Wu, Z.; Cui, Q.; Yethiraj, A. A new coarse-grained model for water: the importance of electrostatic interactions. *J. Phys. Chem. B* **2010**, *114*, 10524–10529.
- (14) Bennett, W. F.; MacCallum, J. L.; Tieleman, D. P. Thermodynamic analysis of the effect of cholesterol on dipalmitoylphosphatidylcholine lipid membranes. *J. Am. Chem. Soc.* **2009**, *131*, 1972–1978.
- (15) Sapay, N.; Bennett, W. F. D.; Tieleman, D. P. Molecular Simulations of Lipid flip-flop in the Presence of Model Transmembrane Helices. *Biochemistry* **2010**, *49*, 7665–7673.
- (16) Fuhrmans, M.; Sanders, B. P.; Marrink, S. J.; de Vries, A. H. Effects of bundling on the properties of the SPC water model. *Theor. Chem. Acc.* **2010**, *125*, 335–344.
- (17) Van Der Spoel, D.; Lindahl, E.; Hess, B.; Groenhof, G.; Mark, A. E.; Berendsen, H. J. GROMACS: fast, flexible, and free. *J. Comput. Chem.* **2005**, *26*, 1701–1718.
- (18) Berger, O.; Edholm, O.; Jahnig, F. Molecular dynamics simulations of a fluid bilayer of dipalmitoylphosphatidylcholine at full hydration, constant pressure, and constant temperature. *Biophys. J.* **1997**, *72*, 2002–2013.
- (19) Berendsen, H. J. C.; Postma, J. P. M.; van Gunsteren, W. F.; Hermans, J. In *Intermolecular Forces*; Pullman, B., Ed.; D. Reidel: Dordrecht, The Netherlands, 1981, p 331–342.
- (20) Biltonen, R. L.; Lichtenberg, D. The Use of Differential Scanning Calorimetry as a Tool to Characterize Liposome Preparations. *Chem. Phys. Lipids* **1993**, *64*, 129–142.
- (21) Miyamoto, S.; Kollman, P. A. Settle - an Analytical Version of the Shake and Rattle Algorithm for Rigid Water Models. *J. Comput. Chem.* **1992**, *13*, 952–962.
- (22) Hess, B.; Bekker, H.; Berendsen, H. J. C.; Fraaije, J. G. E. M. LINCS: A linear constraint solver for molecular simulations. *J. Comput. Chem.* **1997**, *18*, 1463–1472.
- (23) Berendsen, H. J. C.; Postma, J. P. M.; Vangunsteren, W. F.; Dinola, A.; Haak, J. R. Molecular-Dynamics with Coupling to an External Bath. *J. Chem. Phys.* **1984**, *81*, 3684–3690.
- (24) Darden, T.; York, D.; Pedersen, L. Particle Mesh Ewald - an N. Log(N) Method for Ewald Sums in Large Systems. *J. Chem. Phys.* **1993**, *98*, 10089–10092.
- (25) Essmann, U.; Perera, L.; Berkowitz, M. L.; Darden, T.; Lee, H.; Pedersen, L. G. A Smooth Particle Mesh Ewald Method. *J. Chem. Phys.* **1995**, *103*, 8577–8593.
- (26) Kumar, S.; Bouzida, D.; Swendsen, R. H.; Kollman, P. A.; Rosenberg, J. M. The Weighted Histogram Analysis Method for Free-Energy Calculations on Biomolecules 0.1. The Method. *J. Comput. Chem.* **1992**, *13*, 1011–1021.
- (27) Dorairaj, S.; Allen, T. W. On the thermodynamic stability of a charged arginine side chain in a transmembrane helix. *Proc. Natl. Acad. Sci. U.S.A.* **2007**, *104*, 4943–4948.
- (28) MacCallum, J. L.; Bennett, W. F.; Tieleman, D. P. Distribution of amino acids in a lipid bilayer from computer simulations. *Biophys. J.* **2008**, *94*, 3393–3404.
- (29) de Vries, A. H.; Mark, A. E.; Marrink, S. J. Molecular Dynamics Simulation of the Spontaneous Formation of a Small DPPC Vesicle in Water in Atomistic Detail. *J. Am. Chem. Soc.* **2004**, *126*, 4488–4489.
- (30) Johansson, A.; Lindahl, E. Titratable Amino Acid Solvation in Lipid Membranes as a Function of Protonation State. *J. Phys. Chem. B* **2009**, *113*, 245–253.

- (31) Li, L.; Vorobyov, I.; Allen, T. Potential of mean force and pKa profile calculation for a lipid membrane-exposed arginine side chain. *J. Phys. Chem. B.* **2008**, *112*, 9574–9587.
- (32) Yoo, J.; Cui, Q. Does arginine remain protonated in the lipid membrane? Insights from microscopic pKa calculations. *Biophys. J.* **2008**, *94*, L61–63.
- (33) Wu, Z.; Cui, Q.; Yethiraj, A. A New Coarse-Grained Model for Water: The Importance of Electrostatic Interactions. *J. Phys. Chem. B* **2010**, *114*, 10524–10529.
- (34) Brandt, Erik G.; Braun, Anthony R.; Sachs, Jonathan N.; Nagle, John F.; Edholm, O. Interpretation of Fluctuation Spectra in Lipid Bilayer Simulations. *Biophys. J.* **2011**, *100*, 2104–2111.
- (35) Blok, M. C.; Van Der Neut-Kok, E. C. M.; Van Deenen, L. L. M.; De Gier, J. The effect of chain length and lipid phase transitions on the selective permeability properties of liposomes. *Biochim. Biophys. Acta, Biomembr.* **1975**, *406*, 187–196.
- (36) Paula, S.; Volkov, A. G.; Van Hoek, A. N.; Haines, T. H.; Deamer, D. W. Permeation of protons, potassium ions, and small polar molecules through phospholipid bilayers as a function of membrane thickness. *Biophys. J.* **1996**, *70*, 339–348.
- (37) Lee, H.; Larson, R. G. Coarse-grained molecular dynamics studies of the concentration and size dependence of fifth- and seventh-generation PAMAM dendrimers on pore formation in DMPC bilayer. *J. Phys. Chem. B* **2008**, *112*, 7778–7784.
- (38) Rzepiela, A. J.; Sengupta, D.; Goga, N.; Marrink, S. J. Membrane poration by antimicrobial peptides combining atomistic and coarse-grained descriptions. *Faraday Discuss.* **2010**, *144*, 431–443 discussion 445–481.